UDC 621.396.96 **doi: 10.32620/reks.2025.4.17**

Volodymyr PAVLIKOV[1], Maksym PERETIATKO[1], Volodymyr TROFYMENKO[2], Denys KOLESNIKOV[1]

[1] ***State Scientific and Research Institute of Cybersecurity Technologies and Information Protection, Kyiv, Ukraine***

[2] ***State Service of Special Communications and Information Protection of Ukraine, Kyiv, Ukraine***

ESTIMATION OF RADIO PULSE PARAMETERS WITH LINEAR FREQUENCY MODULATION

*The **subject of this** article is the process of estimating the parameters of a pulse signal with linear frequency modulation (LFM) used in airborne radar systems, particularly in synthetic aperture radars (SAR). The **goal** of this study is to synthesize algorithms for the optimal estimation of the key parameters of an LFM signal (i.e., carrier frequency, modulation frequency change rate, pulse length, and radio pulse envelope) and to develop a block diagram of a radar receiver that implements these algorithms. The **tasks** to be solved are as follows: build a mathematical model of a signal with linear frequency modulation emitted by a radar, an observation equation, and a likelihood functional; synthesize algorithms for estimating the parameters of an LFM signal using the maximum likelihood method; and develop a block diagram of a receiver based on the synthesized algorithms. The solutions to these tasks are based on **the** statistical theory of radio engineering systems and computer simulation. The following **results** were obtained: 1) algorithms for estimating the carrier frequency, frequency change rate, pulse length, and radio pulse envelope were synthesized; 2) simulations showed high noise robustness of the algorithms (up to a signal-to-noise ratio of –30 dB); 3) a block diagram of the radar was designed, which implements the synthesized algorithms and refines the estimated parameters in feedback. **Conclusions**. The scientific novelty of the obtained results is as follows: algorithms for estimating the parameters of both the point (carrier frequency, modulation frequency change rate, pulse length) and time characteristics (radio pulse envelope) of pulse LFM signals have been obtained using the maximum likelihood method. For the first time, it has been shown that estimating the pulse width requires solving a transcendental equation, and estimating the envelope requires smoothing in a sliding window. The obtained results expand the application of the maximum likelihood method in signal parameter estimation theory. The theory of phantomization of radio images has been further developed in terms of designing the receiving paths of phantomization radars.*

Keywords: *pulse parameters; linear frequency modulation; likelihood method; phantomization radar; synthetic aperture radar.*

1. Introduction

1.1 Motivation

Studies [1, 2] initiated the development of the theory of radio image phantomization, which is formed by onboard synthetic aperture radar (SAR) [3, 4]. In particular, the general concept of phantomization, which involves making guided changes to the onboard SAR radio image in the form of objects not located in a given area, was proposed and justified [1]. Such object addition is performed by mixing additional phantomization radar signals with the signals reflected by the underlying surface. It is possible to add signals that imitate objects if the SAR waveform is precisely known. Preliminary calculations of the expected SAR signal waveform depending on the underlying surface sensing geometry are justified in [1]. This information is crucial for designing receiving channels in radar systems [2].

However, the principles of optimal estimation algorithm synthesis must be studied, assuming that the estimated parameters and characteristics differ from those in classical radar. To solve the phantomization radar receiver design problem, the carrier frequency, modulation frequency change rate for linear frequency modulation (LFM) signals [5], pulse duration, and pulse envelope must be optimally estimated. The first three parameters are fixed (unchanged for a pulse), whereas the fourth parameter, the envelope of a radio pulse, is a time-dependent characteristic.

ISSN 1814-4225 (print)
ISSN 2663-2012 (online)

Similar knowledge about signal waveforms is also important for solving other radio engineering problems. Such tasks include monitoring the use of radio medium [6], providing secure communication systems [7], designing and implementing radar signal analysis systems for friend-or-foe identification [8], and researching signal propagation paths in space [9].

1.2 State of the art

Classic approach. Various optimization methods can be used to solve this problem: according to the classical scientific works [10, 11], the maximum likelihood method is used to estimate the signal parameters. Practical methods for implementing such estimators in radar systems [12] are based on matched filtering and correlation algorithms that provide combined estimation of time delay and Doppler shift for LFM signals. Notably, the robust algorithm synthesis of signal parameter estimation is well established under conditions of a priori uncertainty by the maximum likelihood method [13, 14].

At the same time, the classical literature lacks comprehensive information on estimating all parameters of LFM signals. However, since these signals are used in many types of modern civil and military radio-electronic systems [15, 16], their detection and parameter estimation are relevant scientific issues.

Fractional transform methods. Currently, there are several relevant studies on determining the LFM signal parameters. However, an analysis of these studies shows that researchers mostly focus on finding only one parameter, specifically the change rate of the modulation frequency. Thus, the review [17] noted the growing trend of using fractional Fourier transform (FrFT) in the analysis of LFM signals because the kernel of the FrFT is constituted by chirp functions. In [18], the authors used the analysis of the peak magnitude of the FrFT and optimization procedures to increase the accuracy of the modulation frequency change. The continuous development of these methods indicates their relevance. For example, in [19], in addition to FrFT, the authors propose using second-order synchrosqueezing transform (SSST) and the Hough transform for increasing energy concentration in the time-frequency domain and obtaining accurate parameter estimation.

Wigner Distribution-based methods. Previous studies [20, 21] have proposed new methods based on Wigner Distribution (WD) associated with linear canonical transforms. Owing to their superior time-frequency localization property, they have found wide application in this area. Thus, [20] proposed a method that achieves results at the level of a closed-form instantaneous cross-correlation function type of WD, allowing the detection of noisy LFM signals under an extremely low SNR while reducing the computational complexity by half.

Compressed sensing-based methods. With the development of the compressed sensing theory, which solves the problem of large-bandwidth signal acquisition, methods for estimating the parameters of compressed LFM signals have gained popularity. Such problems arise during the reconstruction of LFM signals. Thus, [22, 23] proposed methods for estimating the parameters of LFM signals based on the Random Demodulator and Waveform Matching Dictionary and discrete fractional Fourier transform dictionary. The proposed methods show low errors in parameter estimation compared with the original signal and anti-noise performance in general.

Neural network-based approaches. The use of neural networks to solve the problem of estimating the parameters of LFM signals is another promising area. Thus, articles [24, 25] proposed an approach for estimating the initial frequency and modulation frequency change rate based on a neural network to achieve signal denoising and high-resolution spectral line representation, thus estimating the parameters of LFM signals under a low SNR.

However, none of the abovementioned articles solves the problem of estimating multiple parameters optimally within a single method. This does not allow the determination of the marginal errors when using the obtained methods and evaluating their overall efficiency. Additionally, existing works do not consider the design of the radar receiving path for the practical implementation of the obtained algorithms.

Therefore, the optimal algorithm synthesis problem for parameter estimation (carrier frequency, frequency change rate, envelope width, and shape) of an LFM signal is relevant and requires further research. In this study, we propose solving this problem using the maximum likelihood method. The resulting mathematical models will allow us to determine the structure of the radar receiver path and determine the marginal errors of the estimates of the desired parameters in the future, which is important for the implementation of the corresponding radar system.

1.3. Objectives and tasks

The main goal of this study is to synthesize algorithms for the optimal estimation of key LFM signal parameters (i.e., carrier frequency, modulation frequency change rate, pulse length, and radio pulse envelope) and to develop a radar receiver block diagram that implements these algorithms.

To achieve the goal, within the framework of this publication, the following tasks must be solved:

− build a mathematical signal model with linear frequency modulation emitted by a radar, an observation equation, and a likelihood functional;

– synthesize algorithms for estimating the parameters of an LFM signal using the maximum likelihood method;

– develop a receiver block diagram based on the synthesized algorithms.

The remaining part of the article is structured as follows. Section 2 postulates the problem to be solved, mathematically describes the signal, observation equations, and likelihood functional, and sets the vector for further obtaining parameter estimation algorithms. Section 3 is devoted to obtaining algorithms for estimating the parameters of the LFM signal by solving equations obtained by the maximum likelihood method. Sections 4 and 5 conclude the paper by summarizing the obtained estimation algorithms and presenting the paper's theoretical and practical significance, as well as its contribution to the development of radio image phantomization theory.

1.4. Methodology

In this work, the maximum likelihood method is used to synthesize algorithms for parameter estimation of a pulse signal with linear frequency modulation. The signal form, the observation equation at the receiver input (as the sum of the received signal and white Gaussian noise), and the likelihood functional are determined. The algorithm for estimating signal parameters is obtained by evaluating the partial and functional derivatives of the logarithm of the likelihood function, assuming that the parameter estimates coincide with the true values. The reliability of the proposed algorithms was verified by computer simulation in the MATLAB environment. A block diagram of the radar receiving channel has been developed based on the obtained algorithms.

2. Materials and Methods of Research

Problem statement. Synthesis of algorithms for parameter estimation (carrier frequency, frequency change rate, envelope width, and shape) of an LFM signal and development of a radar receiver block diagram are necessary.

2.1. Signal, observation and likelihood functional

Let's write the LFM signal emitted by the radar in the following form

$$s(t)=\mathrm{Re}\exp\left(j\pi\frac{\Delta F}{\tau}t^2\right)\exp(j2\pi f_0 t)\Pi\left(\frac{t}{\tau_p}\right), \quad (1)$$

where $\Pi\left(t/\tau_p\right)$ is the radio pulse envelope, ΔF is the frequency deviation, f_0 is the carrier frequency, τ_p is the envelope length (which can be measured at different levels for different envelope types), t is the time, and τ is the modulation period.

To develop the receiver design, the optimization problem is solved using the maximum likelihood method. Let us write down the observation equation at the receiver input, considering the noise applied to the receiver input:

$$u(t)=s(t)+n(t), \quad (2)$$

where $n(t)$ is a white Gaussian noise with a power spectral density $\frac{N_0}{2}$, zero mean $\langle n(t)\rangle=0$, and correlation function $R_n(t_1-t_2)=\frac{N_0}{2}\delta(t_1-t_2)$. Here $\langle\cdot\rangle$ is the statistical averaging operator.

Let's write the likelihood functional in the general form

$$p(u(t)|\vec{\lambda})=k(\vec{\lambda})\exp\left\{-\iint\left(u(t_1)-\langle u(t_1)\rangle\right)\times W(t_1,t_2)\left(u(t_2)-\langle u(t_2)\rangle\right)dt_1dt_2\right\}, \quad (3)$$

where $W(t_1,t_2)$ is a function inverse to the correlation function of the process $u(t)-\langle u(t)\rangle$, $k(\vec{\lambda})$ is a parameter that may or may not depend on the desired signal parameters, and $\vec{\lambda}$ is a vector of estimated signal parameters, which in this case is $\vec{\lambda}=\left[f_0,\frac{\Delta F}{\tau},\tau_p,\Pi\left(\frac{t}{\tau_p}\right)\right]$.

In a given problem, $\langle u(t)\rangle=\langle s(t)+n(t)\rangle=\langle s(t)\rangle+\langle n(t)\rangle=s(t)$, where $\langle s(t)\rangle=s(t)$ is due to a deterministic waveform. Then the function $W(t_1,t_2)$ is calculated for the noise component of $n(t)$, i.e., $W_n(t_1,t_2)$.

Let's find $W(t_1,t_2)$ from the inverse equation

$$\int R_n(t_1,t)W_n(t,t_2)dt=\delta(t_1-t_2), \quad (4)$$

The solution to equation (4) is obtained directly by substituting the correlation function

ISSN 1814-4225 (print)
ISSN 2663-2012 (online)

$$R_n(t_1-t_2)=\frac{N_0}{2}\delta(t_1-t_2)$$

$$\frac{N_0}{2}\int\delta(t_1-t)W_n(t,t_2)dt=\delta(t_1-t_2),$$

or

$$W_n(t_1,t_2)=\frac{2}{N_0}\delta(t_1-t_2). \quad (5)$$

Substituting (5) into (3), we can write the likelihood functional with an accuracy of $k(\vec{\lambda})$ (the derivative of $k(\vec{\lambda})$, not the parameter itself, has a physical essence)

$$\begin{aligned}p(u(t)|\vec{\lambda})&=k(\vec{\lambda})\exp\left\{-\frac{2}{N_0}\iint\left(u(t_1)-s(t_1,\vec{\lambda})\right)\times\right.\\&\left.\times\delta(t_1-t_2)\left(u(t_2)-s(t_2,\vec{\lambda})\right)dt_1dt_2\right\}=\\&=k(\vec{\lambda})\exp\left\{-\frac{2}{N_0}\int\left(u(t)-s(t,\vec{\lambda})\right)^2dt\right\}.\end{aligned} \quad (6)$$

2.2. Problem solution

Let's find the optimal processing algorithms using the maximum likelihood method. To do so, let's solve the system of equations (7).

$$\begin{cases}\dfrac{\partial}{\partial\frac{\Delta F}{\tau}}\ln p\left(\begin{matrix}u(t)|\frac{\Delta F}{\tau},f_0,\\ \tau_p,\Pi\left(\frac{t}{\tau_p}\right)\end{matrix}\right)\Bigg|_{\frac{\Delta\hat{F}}{\tau}=\left(\frac{\Delta F}{\tau}\right)_{true}}=0,\\ \dfrac{\partial}{\partial f_0}\ln p\left(u(t)|\frac{\Delta F}{\tau},f_0,\tau_p,\Pi\left(\frac{t}{\tau_p}\right)\right)\Bigg|_{\hat{f}_0=f_{0,true}}=0,\\ \dfrac{\partial}{\partial\tau_p}\ln p\left(u(t)|\frac{\Delta F}{\tau},f_0,\tau_p,\Pi\left(\frac{t}{\tau_p}\right)\right)\Bigg|_{\hat{\tau}_p=\tau_{p,true}}=0,\\ \dfrac{\delta}{\delta\Pi\left(\frac{t}{\tau_p}\right)}\ln p\left(\begin{matrix}u(t)|\frac{\Delta F}{\tau},f_0,\\ \tau_p,\Pi\left(\frac{t}{\tau_p}\right)\end{matrix}\right)\Bigg|_{\hat{\Pi}(\cdot)=\Pi_{true}(\cdot)}=0,\end{cases} \quad (7)$$

We also consider the received signal phase to be unknown. Therefore, based on known solutions, we will use a module of synthesized signal processing algorithms. In (7), we use the notation $\frac{\partial}{\partial\lambda}$ and $\frac{\delta}{\delta\Pi(\cdot)}$, respectively, for the partial and functional derivative operators, respectively.

The partial derivatives for each of the desired signal parameters are found, and the corresponding processing algorithms are obtained. Each algorithm is used to design the corresponding radar channel.

3. Results

3.1. $\frac{\Delta F}{\tau}$ estimation algorithm

The $\frac{\Delta F}{\tau}$ estimation algorithm can be determined by solving the first equation of the system (7). This and other algorithms will depend on other estimated parameters; therefore, we should have a priori (approximate) information about other parameters before all channels receive parameter estimates.

Let us substitute the likelihood functional (6) into the first equation of the system (7) and solve it

$$\begin{aligned}&\frac{\partial}{\partial\frac{\Delta F}{\tau}}\ln k(\vec{\lambda})-\frac{2}{N_0}\times\\&\times\int\frac{\partial}{\partial\frac{\Delta F}{\tau}}\left(u(t)-s\left(t,\frac{\Delta F}{\tau}\right)\right)^2dt\Bigg|_{\frac{\Delta\hat{F}}{\tau}=\left(\frac{\Delta F}{\tau}\right)_{true}}=0,\end{aligned} \quad (8)$$

where

$$\begin{aligned}&\frac{\partial}{\partial\frac{\Delta F}{\tau}}\ln k(\vec{\lambda})=\\&=\iint\left[\frac{\partial}{\partial\frac{\Delta F}{\tau}}R_n(t_1-t_2)\right]W_n(t_1-t_2)dt_1dt_2=\\&=\frac{N_0}{2}\iint\left[\frac{\partial}{\partial\frac{\Delta F}{\tau}}\delta(t_1-t_2)\right]W_n(t_1-t_2)dt_1dt_2=0,\end{aligned} \quad (9)$$

Considering (9) and calculating the derivative of the second component of (8), we obtain

$$-\frac{4}{N_0}\int\left(u(t)-s\left(t,\frac{\Delta F}{\tau}\right)\right)\frac{\partial}{\partial\frac{\Delta F}{\tau}}s\left(t,\frac{\Delta F}{\tau}\right)dt=0, \quad (10)$$

or

$$\begin{aligned}&\int u(t)\frac{\partial}{\partial\frac{\Delta F}{\tau}}s\left(t,\frac{\Delta F}{\tau}\right)dt=\\&=\int s\left(t,\frac{\Delta F}{\tau}\right)\frac{\partial}{\partial\frac{\Delta F}{\tau}}s\left(t,\frac{\Delta F}{\tau}\right)dt,\end{aligned} \quad (11)$$

In (11), the left and right parts are equated but not equal. The equality between them will occur when calculating the expected value (mean) of the left part, i.e.

$$\left\langle \int u(t)\frac{\partial}{\partial\frac{\Delta F}{\tau}}s\left(t,\frac{\Delta F}{\tau}\right)dt\right\rangle = \int\left\langle u(t)\right\rangle\frac{\partial}{\partial\frac{\Delta F}{\tau}}s\left(t,\frac{\Delta F}{\tau}\right)dt = \left|\left\langle u(t)\right\rangle = \left\langle s\left(t,\frac{\Delta F}{\tau}\right)+n(t)\right\rangle = s\left(t,\frac{\Delta F}{\tau}\right)\right| = \int s\left(t,\frac{\Delta F}{\tau}\right)\frac{\partial}{\partial\frac{\Delta F}{\tau}}s\left(t,\frac{\Delta F}{\tau}\right)dt. \quad (12)$$

Let's find $\frac{\partial}{\partial\frac{\Delta F}{\tau}}s\left(t,\frac{\Delta F}{\tau}\right)$ (substitute the signal (1) under the derivative sign)

$$\frac{\partial}{\partial\frac{\Delta F}{\tau}}s\left(t,\frac{\Delta F}{\tau}\right) = \mathrm{Re}\frac{\partial}{\partial\frac{\Delta F}{\tau}}\exp\left(j\pi\frac{\Delta F}{\tau}t^2\right)\times \times\exp\left(j2\pi f_0 t\right)\Pi\left(\frac{t}{\tau_p}\right) =$$

$$= \pi t^2\Pi\left(\frac{t}{\tau_p}\right)\mathrm{Re}\, j\exp\left(j\pi\frac{\Delta F}{\tau}t^2\right)\exp\left(j2\pi f_0 t\right) =$$

$$= \pi t^2\Pi\left(\frac{t}{\tau_p}\right)\mathrm{Re}\, j\left[\cos\left(\pi\frac{\Delta F}{\tau}t^2\right)+j\sin\left(\pi\frac{\Delta F}{\tau}t^2\right)\right]\times \times\left[\cos\left(2\pi f_0 t\right)+j\sin\left(2\pi f_0 t\right)\right] =$$

$$= \pi t^2\Pi\left(\frac{t}{\tau_p}\right)\mathrm{Re}\begin{bmatrix} j\cos\left(\pi\frac{\Delta F}{\tau}t^2\right)\cos\left(2\pi f_0 t\right)- \\ -\cos\left(\pi\frac{\Delta F}{\tau}t^2\right)\sin\left(2\pi f_0 t\right)- \\ -\sin\left(\pi\frac{\Delta F}{\tau}t^2\right)\cos\left(2\pi f_0 t\right)- \\ -j\sin\left(\pi\frac{\Delta F}{\tau}t^2\right)\sin\left(2\pi f_0 t\right)\end{bmatrix} =$$

$$= -\pi t^2\Pi\left(\frac{t}{\tau_p}\right)\begin{bmatrix}\cos\left(\pi\frac{\Delta F}{\tau}t^2\right)\sin\left(2\pi f_0 t\right)+ \\ +\sin\left(\pi\frac{\Delta F}{\tau}t^2\right)\cos\left(2\pi f_0 t\right)\end{bmatrix} =$$

$$= -\pi t^2\Pi\left(\frac{t}{\tau_p}\right)\sin\left(2\pi t\left(f_0+\frac{1}{2}\frac{\Delta F}{\tau}t\right)\right). \quad (13)$$

Substituting (13) into the right part of (11)

$$\int s\left(t,\frac{\Delta F}{\tau}\right)\frac{\partial}{\partial\frac{\Delta F}{\tau}}s\left(t,\frac{\Delta F}{\tau}\right)dt = -\pi\int t^2\Pi^2\left(\frac{t}{\tau_p}\right)\cos\left(2\pi t\left(f_0+\frac{1}{2}\frac{\Delta F}{\tau}t\right)\right)\times \times\sin\left(2\pi t\left(f_0+\frac{1}{2}\frac{\Delta F}{\tau}t\right)\right)dt = 0. \quad (14)$$

Following (14), the algorithm for optimal $\frac{\Delta F}{\tau}$ estimation is written as follows, which, considering the unknown phase of the received signal, is calculated using the output effect modulus (in this case, we proceed to the maximum instead of the minimum of the output effect):

$$\left|\int t^2\Pi\left(\frac{t}{\tau_p}\right)u(t)\exp\left(j2\pi t\left(f_0+\frac{1}{2}\frac{\Delta F}{\tau}t\right)\right)dt\right| = \max. \quad (15)$$

Note that the algorithm (15) is designed for the case of parity between the received signal and the reference signal derivative. The output effect as a mismatch function for the desired parameter $\frac{\Delta F}{\tau}$ is also informative, i.e., the function

$$Y_{out}(\gamma) = \left|\int t^2\Pi\left(\frac{t}{\tau_p}\right)u(t)\times \times\exp\left(j2\pi t\left(f_0+\frac{1}{2}\left(\frac{\Delta F}{\tau}+\gamma\right)t\right)\right)dt\right|. \quad (16)$$

Fig. 1 shows a diagram of the output effect $Y_{out}(\gamma)$ obtained for the following input data: $\frac{\Delta F}{\tau} = \frac{100\cdot 10^6}{10\cdot 10^{-6}} = 10\cdot 10^{12}$, $f_0 = 100$ MHz, $t = 0..\tau$, with a signal-to-noise ratio (at the input) of -16,8 dB.

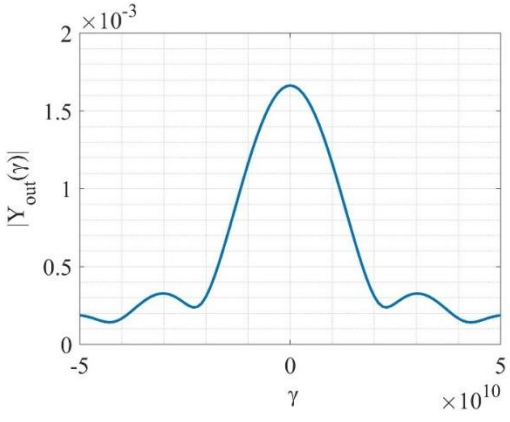

Fig. 1. Output effect $Y_{out}(\gamma)$

ISSN 1814-4225 (print)
ISSN 2663-2012 (online)

Analysis of Fig. 1 shows that the maximum can be unambiguously estimated and, therefore, measure the $\frac{\Delta F}{\tau}$ value. The impact of the error γ on the output effect is negligible because it is more than twice as small as $\frac{\Delta F}{\tau}$.

3.2. f_0 estimation algorithm

Similar to the previous case, we synthesize the f_0 estimation algorithm from the solution of the second equation of the system (7).

Substituting the likelihood functional (6) into the second equation of system (7) and solve

$$\left.\begin{aligned}&\frac{\partial}{\partial f_0}\ln k\left(\vec{\lambda}\right)-\frac{2}{N_0}\times\\ &\times\int\frac{\partial}{\partial f_0}\left(u(t)-s(t,f_0)\right)^2dt\end{aligned}\right|_{\hat{f}_0=f_{0,true}}=0, \qquad (17)$$

where

$$\begin{aligned}&\frac{\partial}{\partial f_0}\ln k\left(\vec{\lambda}\right)=\\ &=\iint\left[\frac{\partial}{\partial f_0}R_n(t_1-t_2)\right]W_n(t_1-t_2)dt_1dt_2=\\ &=\frac{N_0}{2}\iint\left[\frac{\partial}{\partial f_0}\delta(t_1-t_2)\right]W_n(t_1-t_2)dt_1dt_2=0.\end{aligned} \qquad (18)$$

Now let's find the derivative of the second term (18)

$$-\frac{4}{N_0}\int\left(u(t)-s(t,f_0)\right)\frac{\partial}{\partial f_0}s(t,f_0)dt=0,$$

or similar to (11)

$$\int u(t)\frac{\partial}{\partial f_0}s(t,f_0)dt=\int s(t,f_0)\frac{\partial}{\partial f_0}s(t,f_0)dt. \qquad (19)$$

As in (12), the left and right sides are equated.

Let's find $\frac{\partial}{\partial f_0}s(t,f_0)$ (substitute the signal (1) for the derivative)

$$\begin{aligned}&\frac{\partial}{\partial f_0}s(t,f_0)=\mathrm{Re}\exp\left(j\pi\frac{\Delta F}{\tau}t^2\right)\frac{\partial}{\partial f_0}\times\\ &\times\exp\left(j2\pi f_0t\right)\Pi\left(\frac{t}{\tau_p}\right)=\\ &=j2\pi t\,\Pi\left(\frac{t}{\tau_p}\right)\mathrm{Re}\,j\exp\left(j\pi\frac{\Delta F}{\tau}t^2\right)\exp\left(j2\pi f_0t\right)=\\ &=-2\pi t\,\Pi\left(\frac{t}{\tau_p}\right)\sin\left(2\pi t\left(f_0+\frac{1}{2}\frac{\Delta F}{\tau}t\right)\right).\end{aligned} \qquad (20)$$

Substituting (20) into the right part of (19)

$$\begin{aligned}&\int s(t,f_0)\frac{\partial}{\partial f_0}s(t,f_0)dt=\\ &=-2\pi\int t\Pi^2\left(\frac{t}{\tau_p}\right)\cos\left(2\pi t\left(f_0+\frac{1}{2}\frac{\Delta F}{\tau}t\right)\right)\times\\ &\times\sin\left(2\pi t\left(f_0+\frac{1}{2}\frac{\Delta F}{\tau}t\right)\right)dt=0.\end{aligned} \qquad (21)$$

Then, according to (21), we find the algorithm for optimal f_0 estimation in the form as follows

$$\left|\int t\,\Pi\left(\frac{t}{\tau_p}\right)u(t)\exp\left(j2\pi t\left(f_0+\frac{1}{2}\frac{\Delta F}{\tau}t\right)\right)dt\right|=\max. \qquad (22)$$

As in (15), the output effect modulus is used to average the received signal in phase.

Similar to (16), we consider that the algorithm (22) is designed for the case of an exact time match between the received signal and the derivative of the reference signal. Therefore, it is informative to analyze the output effect as a function of the mismatch in f_0, i.e.

$$\begin{aligned}&Y_{out}(\phi)=\left|\int t\,\Pi\left(\frac{t}{\tau_p}\right)u(t)\times\right.\\ &\left.\times\exp\left(j2\pi t\left(\left(f_0+\phi\right)+\frac{1}{2}\frac{\Delta F}{\tau}t\right)\right)dt\right|.\end{aligned} \qquad (23)$$

Fig. 2 shows the graph of the output effect $Y_{out}(\phi)$ obtained for the input data used for the diagram in Fig. 1.

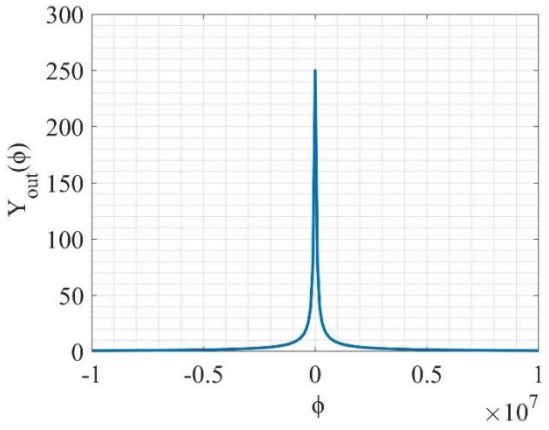

Fig. 2. Output effect $Y_{out}(\phi)$

Analysis of Fig. 2 shows that the estimate is unambiguous.

3.3. τ_p estimation algorithm

The τ_p estimation algorithm is derived from the solution of the third equation of the system (7).

Substituting the likelihood functional (6) into the third equation of system (7)

$$\left.\frac{\partial}{\partial\tau_p}\ln k\left(\vec{\lambda}\right)-\frac{2}{N_0}\times\right.$$
$$\left.\times\int\frac{\partial}{\partial\tau_p}\left(u(t)-s\left(t,\tau_p\right)\right)^2dt\right|_{\hat{\tau}_p=\tau_{p,true}}=0, \qquad (24)$$

where

$$\frac{\partial}{\partial\tau_p}\ln k\left(\vec{\lambda}\right)=$$
$$=\iint\left[\frac{\partial}{\partial\tau_p}R_n\left(t_1-t_2\right)\right]W_n\left(t_1-t_2\right)dt_1dt_2= \qquad (25)$$
$$=\frac{N_0}{2}\iint\left[\frac{\partial}{\partial\tau_p}\delta\left(t_1-t_2\right)\right]W_n\left(t_1-t_2\right)dt_1dt_2=0.$$

Derivative of the second term in (24)

$$-\frac{4}{N_0}\int\left(u(t)-s\left(t,\tau_p\right)\right)\frac{\partial}{\partial\tau_p}s\left(t,\tau_p\right)dt=0,$$

or similar to (11)

$$\int u(t)\frac{\partial}{\partial\tau_p}s\left(t,\tau_p\right)dt=\int s\left(t,\tau_p\right)\frac{\partial}{\partial\tau_p}s\left(t,\tau_p\right)dt. \qquad (26)$$

The left and right sides are equated as in (12) and (19).

To find the derivative of $\frac{\partial}{\partial\tau_p}s\left(t,\tau_p\right)$, it is reasonable to mathematically formalize $\Pi\left(\frac{t}{\tau_p}\right)$ in the signal (1). For example, a Gaussian envelope of the pulse can be introduced, i.e.

$$\Pi\left(\frac{t}{\tau_p}\right)=\exp\left(-\frac{2(t-0.5\tau)^2}{\tau_p^2}\right).$$

Then the derivative

$$\frac{\partial}{\partial\tau_p}s\left(t,\tau_p\right)=\operatorname{Re}\exp\left(j\pi\frac{\Delta F}{\tau}t^2\right)\times$$
$$\times\exp\left(j2\pi f_0t\right)\frac{\partial}{\partial\tau_p}\exp\left(-\frac{2(t-\tau)^2}{\tau_p^2}\right)=$$
$$=\frac{4(t-\tau)^2}{\tau_p^3}\exp\left(-\frac{2(t-\tau)^2}{\tau_p^2}\right)\times$$
$$\times\operatorname{Re}\exp\left(j\pi\frac{\Delta F}{\tau}t^2\right)\exp\left(j2\pi f_0t\right)= \qquad (27)$$
$$=\frac{4(t-\tau)^2}{\tau_p^3}\exp\left(-\frac{2(t-\tau)^2}{\tau_p^2}\right)\cos\left(2\pi t\left(f_0+\frac{1}{2}\frac{\Delta F}{\tau}t\right)\right).$$

Substituting (27) into the right part of (26)

$$\int s\left(t,\tau_p\right)\frac{\partial}{\partial\tau_p}s\left(t,\tau_p\right)dt=$$
$$=\frac{4}{\tau_p^3}\int(t-\tau)^2\exp\left(-\frac{4(t-\tau)^2}{\tau_p^2}\right)\times$$
$$\times\cos^2\left(2\pi t\left(f_0+\frac{1}{2}\frac{\Delta F}{\tau}t\right)\right)dt=$$
$$=\frac{2}{\tau_p^3}\int(t-\tau)^2\exp\left(-\frac{4(t-\tau)^2}{\tau_p^2}\right)\times$$
$$\times\left(1+\cos^2\left(4\pi t\left(f_0+\frac{1}{2}\frac{\Delta F}{\tau}t\right)\right)\right)dt\approx \qquad (28)$$
$$\approx\frac{2}{\tau_p^3}\int(t-\tau)^2\exp\left(-\frac{4(t-\tau)^2}{\tau_p^2}\right)dt.$$

Here is the algorithm for optimal τ_p estimation in the following form:

$$\int(t-\tau)^2\exp\left(-\frac{2(t-\tau)^2}{\tau_p^2}\right)u(t)\times$$
$$\times\cos\left(2\pi t\left(f_0+\frac{1}{2}\frac{\Delta F}{\tau}t\right)\right)dt=$$
$$=\frac{1}{2}\int(t-\tau)^2\exp\left(-\frac{4(t-\tau)^2}{\tau_p^2}\right)dt.$$

The right side is one of the possible expressions of the function width.

The output effect module is used for the phase averaging of the received signal:

$$\left|\int(t-\tau)^2\exp\left(-\frac{2(t-\tau)^2}{\tau_p^2}\right)u(t)\times\right.$$
$$\left.\times\exp\left(j2\pi t\left(f_0+\frac{1}{2}\frac{\Delta F}{\tau}t\right)\right)dt\right|= \qquad (29)$$
$$=\frac{1}{2}\int(t-\tau)^2\exp\left(-\frac{4(t-\tau)^2}{\tau_p^2}\right)dt.$$

ISSN 1814-4225 (print)
ISSN 2663-2012 (online)

As shown in (29), the decision on the pulse width is made by equating the left and right parts (equality occurs when the left part is averaged and the width of the envelope signal in the observation and reference signals is matched).

Let us form two mismatch functions, one for the left part and one for the right part, and equate them to each other. At the matching point, a decision is made regarding the width:

$$Y_{out}(\xi)=\left|\int (t-\tau)^2 \exp\left(-\frac{2(t-\tau)^2}{(\tau_p-\xi)^2}\right)u(t)\times\right.$$
$$\left.\times\exp\left(j2\pi t\left(f_0+\frac{1}{2}\frac{\Delta F}{\tau}t\right)\right)dt\right|; \quad (30)$$
$$Y_{out,ref}(\xi)=\frac{1}{2}\int (t-\tau)^2 \exp\left(-\frac{4(t-\tau)^2}{(\tau_p-\xi)^2}\right)dt;$$
$$Y_{out}(\xi)=Y_{out,ref}(\xi).$$

Fig. 3 shows the diagrams of the output effects $Y_{out}(\xi)$ and $Y_{out,ref}(\xi)$ obtained for the input data used to make the diagram in Fig. 1. Analysis of Fig. 3 shows that at the point of true value (at point $\xi=0$), the output effects intersect.

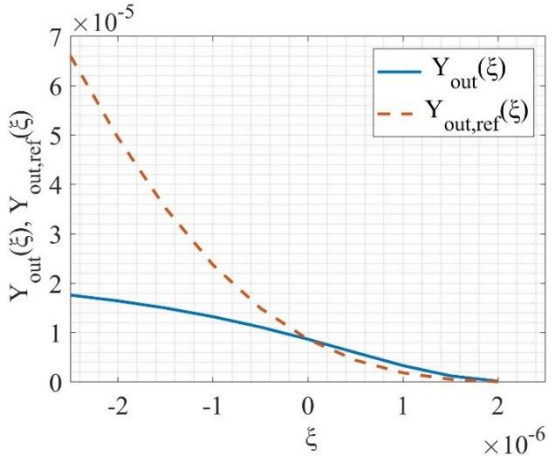

Fig. 3. Output effects $Y_{out}(\xi)$ and $Y_{out,ref}(\xi)$

3.4. Estimation of radio pulse envelope

Let us synthesize the envelope estimation algorithm by solving the fourth equation of system (7)

$$\left.\frac{\delta \ln p\left(u(t)\left|\frac{\Delta F}{\tau},f_0,\tau_p,\Pi\left(\frac{t}{\tau_p}\right)\right.\right)}{\delta\Pi\left(\frac{t}{\tau_p}\right)}\right|_{\hat{\Pi}(\cdot)=\Pi_{true}(\cdot)}=0. \quad (31)$$

Substituting the likelihood functional (6) into the third equation of system (7)

$$\left.\frac{\delta}{\delta\Pi\left(\frac{t}{\tau_p}\right)}\ln k\left(\vec{\lambda}\right)-\right.$$
$$\left.-\frac{2}{N_0}\int\frac{\delta\left(u(t)-s\left(t,\Pi\left(\frac{t}{\tau_p}\right)\right)\right)^2}{\delta\Pi\left(\frac{t}{\tau_p}\right)}dt\right|_{\hat{\Pi}(\cdot)=\Pi_{true}(\cdot)}=0, \quad (32)$$

where the correlation function and the inverse correlation function are independent of the envelope function. Thus

$$\frac{\delta}{\delta\Pi\left(\frac{t}{\tau_p}\right)}\ln k\left(\vec{\lambda}\right)= \quad (33)$$
$$=\iint\left[\frac{\delta}{\delta\Pi\left(\frac{t}{\tau_p}\right)}R_n(t_1-t_2)\right]W_n(t_1-t_2)dt_1dt_2=$$
$$=\frac{N_0}{2}\iint\left[\frac{\delta}{\delta\Pi\left(\frac{t}{\tau_p}\right)}\delta(t_1-t_2)\right]W_n(t_1-t_2)dt_1dt_2=0.$$

Derivative of the second term of (32)

$$-\frac{4}{N_0}\int\left(u(t)-s\left(t,\Pi\left(\frac{t}{\tau_p}\right)\right)\right)\frac{\delta s\left(t,\Pi\left(\frac{t}{\tau_p}\right)\right)}{\delta\Pi\left(\frac{t}{\tau_p}\right)}dt=0,$$

or

$$\int u(t)\frac{\delta}{\delta\Pi\left(\frac{t}{\tau_p}\right)}s\left(t,\Pi\left(\frac{t}{\tau_p}\right)\right)dt=$$
$$=\int s\left(t,\Pi\left(\frac{t}{\tau_p}\right)\right)\frac{\delta}{\delta\Pi\left(\frac{t}{\tau_p}\right)}s\left(t,\Pi\left(\frac{t}{\tau_p}\right)\right)dt. \quad (34)$$

The left and right parts are equated to each other.

As before, the envelope is specified as a Gaussian curve $\Pi\left(\frac{t}{\tau_p}\right)=\exp\left(-\frac{2(t-0.5\tau)^2}{\tau_p^2}\right)$. In this case

$$\frac{\delta}{\delta\Pi\left(\frac{t'}{\tau_p}\right)}s\left(t,\Pi\left(\frac{t}{\tau_p}\right)\right)=\mathrm{Re}\exp\left(j\pi\frac{\Delta F}{\tau}t^2\right)\times$$

$$\times\exp\left(j2\pi f_0 t\right)\frac{\delta}{\delta\Pi\left(\frac{t'}{\tau_p}\right)}\exp\left(-\frac{2(t-\tau)^2}{\tau_p^2}\right)=$$

$$=\mathrm{Re}\exp\left(j\pi\frac{\Delta F}{\tau}t^2\right)\exp\left(j2\pi f_0 t\right)\times$$

$$\times\lim_{\alpha\to 0}\frac{d}{d\alpha}\left[\exp\left(-\frac{2(t-\tau)^2}{\tau_p^2}\right)+\alpha\delta(t-t')\right]=$$

$$=\mathrm{Re}\exp\left(j\pi\frac{\Delta F}{\tau}t^2\right)\exp\left(j2\pi f_0 t\right)\delta(t-t'). \quad (35)$$

Substituting (35) into the right part of (34)

$$\int s\left(t,\Pi\left(\frac{t}{\tau_p}\right)\right)\frac{\delta}{\delta\Pi\left(\frac{t}{\tau_p}\right)}s\left(t,\Pi\left(\frac{t}{\tau_p}\right)\right)dt=$$

$$=\int\exp\left(-\frac{2(t-\tau)^2}{\tau_p^2}\right)\cos^2\left(2\pi f_0 t+\pi\frac{\Delta F}{\tau}t^2\right)\delta(t-t')dt=$$

$$=\exp\left(-\frac{2(t-\tau)^2}{\tau_p^2}\right)\cos^2\left(2\pi f_0 t+\pi\frac{\Delta F}{\tau}t^2\right)=$$

$$=\frac{1}{2}\exp\left(-\frac{2(t-\tau)^2}{\tau_p^2}\right)\left[1+\cos\left(4\pi f_0 t+2\pi\frac{\Delta F}{\tau}t^2\right)\right]. \quad (36)$$

The optimal envelope estimation algorithm is as follows

$$u(t)\cos\left(2\pi f_0 t+\pi\frac{\Delta F}{\tau}t^2\right)=$$

$$=\frac{1}{2}\exp\left(-\frac{2(t-\tau)^2}{\tau_p^2}\right)\cos^2\left(2\pi f_0 t+\pi\frac{\Delta F}{\tau}t^2\right),$$

or

$$2\frac{u(t)}{\cos\left(2\pi f_0 t+\pi\frac{\Delta F}{\tau}t^2\right)}=\exp\left(-\frac{2(t-\tau)^2}{\tau_p^2}\right). \quad (37)$$

Overall, (37) can be expressed for any envelope, i.e.

$$\hat{\Pi}\left(\frac{t}{\tau_p}\right)=2\frac{u(t)}{\cos\left(2\pi f_0 t+\pi\frac{\Delta F}{\tau}t^2\right)}. \quad (38)$$

However, to obtain an algorithm for envelope estimation, the following features of the problem must be considered:

− received signal phase is a random value;

− observation $u(t)$ contains noise (see (2)), and therefore, it is necessary to average it, for example, by smoothing in a sliding window, to obtain a consistent estimate.

In this case, (38) should be rewritten as follows:

$$\hat{\Pi}\left(\frac{t}{\tau_p}\right)=$$

$$=2\left|\int u(t')\exp\left(-j2\pi f_0 t'-j\pi\frac{\Delta F}{\tau}(t')^2\right)w(t-t')dt'\right|. \quad (39)$$

Here, the sliding window function $w(t)$ should be much shorter than τ_p and contain many noise samples to achieve the averaging effect.

For the case of a non-point parameter, the mismatch function is written as follows

$$Y_{out}(t,\phi,\xi)=$$

$$=2\left|\int u(t')\exp\left(\begin{matrix}-j2\pi(f_0-\phi)t'-\\-j\pi\left(\frac{\Delta F}{\tau}-\xi\right)(t')^2\end{matrix}\right)g(t-t')dt'\right|. \quad (40)$$

Since the function depends on three parameters, it is advisable to analyze the estimation error by fixating one of the parameters ϕ or ξ.

Fig. 4 shows the result of estimating the envelope according to (39).

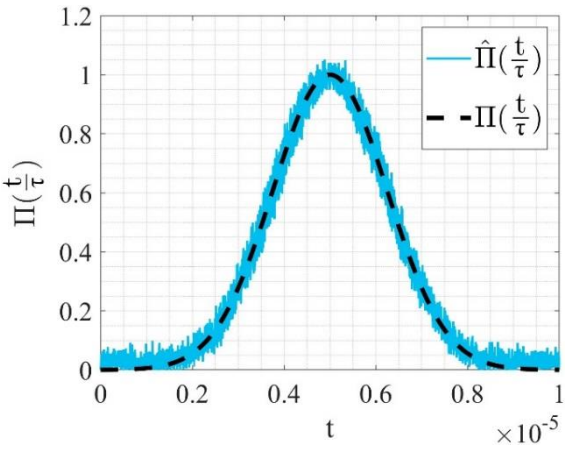

Fig. 4. The envelope $\Pi\left(\frac{t}{\tau_p}\right)$ and its estimate $\hat{\Pi}\left(\frac{t}{\tau_p}\right)$

Fig. 4 shows that the estimate agrees well enough with the envelope. Additional smoothing can be

ISSN 1814-4225 (print)
ISSN 2663-2012 (online)

performed to reduce the noise, or the smoothing window in (39) can be expanded.

3.5. Radar block diagram

We develop a radar block diagram following the synthesized algorithms (15), (22), (29), and (39).

Fig. 5 shows a block diagram with the following notations: A is the antenna; In is the receiver input path, which includes low-noise amplifiers and may also contain mixers and low-pass filters (depending on the carrier frequency); $\boxed{\times}$ is the multiplication unit; $\boxed{\otimes}$ is the convolution unit; $\boxed{|\cdot|}$ is the modulus unit; $\boxed{\int dt}$ is the integration unit; $\boxed{\max}$ is the maximum output search unit; $\boxed{\text{Calc}}$ is a unit that selects the envelope among all solutions; $\boxed{\tau}$ is a delay unit; $\triangleright$ is an amplification unit (the gain is specified within the unit); $\boxed{0,5}$ is an attenuator with a 2-fold attenuation; $\boxed{=}$ is a comparison unit; $\boxed{G}$ is an oscillator; $\boxed{\Pi}$ is an envelope (reference) generator; $\boxed{T}$ is a time reference generator of t; $w(t)$ is a window function (for smoothing).

The circuit works as follows. The signal from the output of the antenna A comes to the receiver In input path, where it is amplified and processed depending on the receiver type (tuned radio frequency or superheterodyne type). Then the signal from the antenna and the (complex) signal of the oscillator G are multiplied. Several expected reference values, $\vec{f}_0$ and $\overrightarrow{\frac{\Delta F}{\tau}}$ (used when launching the radar), form the oscillator signal. Information on the corrected values of $\hat{f}_0$ and $\frac{\Delta F}{\tau}$ comes from the outputs of the respective estimation channels, after the estimates are generated, and is used for the entire radar operation time. The envelope estimation channel implements the smoothing of the obtained multiplication in unit $\boxed{\otimes}$ by the window $w(t)$. Then, the modulus is calculated, and the signal envelope estimate $\hat{\Pi}(t/\tau_p)$ is selected in $\boxed{\text{Calc}}$. The f_0 and $\frac{\Delta F}{\tau}$ estimation channels are similar, containing multipliers, integrators, modulus, and maximum output effect calculation units. At the initial stage, information about possible envelope signals ($\boxed{\Pi}$ unit) is entered, the information about which is specified by the $\hat{\Pi}(t/\tau_p)$ estimation. The pulse duration estimation channel $\hat{\tau}_p$, which contains the solution of the transcendental equation (39), multipliers, integrators, an attenuator $\boxed{0.5}$, and a comparison unit $\boxed{=}$. All the parameter estimates are fed through a feedback loop to the corresponding radar blocks and do not affect the signal parameter estimation.

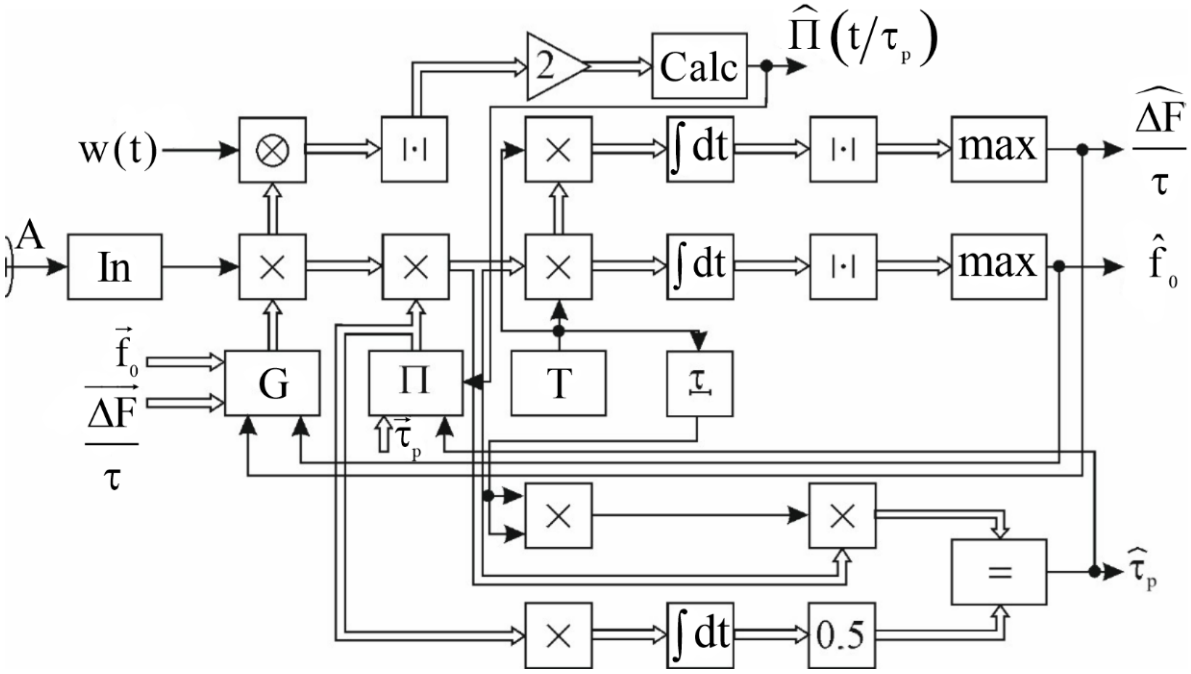

Fig. 5. Radar block diagram

4. Discussion

Based on the analytical expressions obtained for algorithms for estimating LFM radio pulse parameters, the output effects were computer-modeled to estimate the modulation frequency change rate, carrier frequency, pulse width, and envelope.

As shown in Fig. 1 and Fig. 2, for the given signal parameters, the output effect functions have clearly defined maxima when the difference between the desired signal parameter and the signal parameter formed by the system approaches zero. Thus, further research should be conducted to determine potential approaches for forming reference signals under conditions of complete uncertainty and when a priori data on the received signal is available to fully implement the proposed algorithm in an autonomous system.

The results are shown in Fig. 3 indicate that the pulse width is estimated by finding the intersection point of two output effects, which corresponds to the solution of a transcendental equation.

Fig. 4 shows the result of estimating the radio pulse envelope using sliding window smoothing. The obtained estimate agrees with the shape of the given envelope, whereas the presence of noise leads to fluctuations, the level of which can be reduced by increasing the smoothing window length.

The simulation results shown in Figs. 1-4 were obtained considering the receiver noise at a signal-to-noise ratio of -16.8 dB and remained almost unchanged when the signal-to-noise ratio was reduced to -30 dB.

The potential implementation of the radio engineering system is shown in Fig. 5 has high requirements for electronic components. It is necessary to ensure coherent signal reception, its digitization in the full frequency band, and further processing of samples in real or quasi-real time for its effective operation. This requires the use of low-noise radio components in the system's analog path, high-speed analog-to-digital receivers, and hardware implementation of processing in FPGAs or special-purpose integrated circuits. In future works, we will discuss the component base that can be used for implementation.

5. Conclusions

The main contribution of this study is the synthesis of algorithms for estimating the carrier frequency f_0, frequency change rate $\frac{\Delta F}{\tau}$, pulse width τ_p, and envelope $\Pi\left(t/\tau_p\right)$ of the LFM radio pulse using the maximum likelihood method, followed by their implementation in the receiver's block diagram.

The process of obtaining algorithms for optimal signal processing is also methodologically important because the algorithms are synthesized using a single method. However, both point parameters and characteristics (envelope as a function of time) are calculated. This imposes peculiarities on the process of obtaining algorithms and their interpretation. It was shown for the first time that pulse width estimation requires solving the transcendental equation, and envelope estimation necessitates the implementation of additional estimation smoothing using a sliding window, which provides a practical averaging operation that equates the left and right sides of the likelihood equation.

The radar block diagram is developed, and its operating principle is described. It is demonstrated that for the initial parameter estimation, approximate values of these signal parameters are necessary. After obtaining the initial estimates, they should be fed back into the corresponding blocks in a feedback loop for adjustment.

The theoretical significance of this work lies in the development of signal parameter estimation theory through the application of the maximum likelihood method to point parameter and characteristic estimation.

The practical significance of this work lies in the development of algorithms for parameter estimation of a pulse LFM signal and the corresponding radar block diagram.

Theoretical and practical significance contribute to develop the radio image phantomization theory in terms of the design and engineering implementation of the phantomization radar input channel, which is designed to determine the signal packet parameters [1].

Future research directions. Further scientific works should be devoted to the implementation of the developed algorithms and the radar receiver block diagram using modern FPGA-based computing technologies and modern electronic components, as well as the evaluation of the accuracy of LFM radio-pulse parameter estimation.

Contribution of authors: conceptualization – **Volodymyr Pavlikov**, **Maksym Peretiatko**; methodology – **Volodymyr Pavlikov**, **Volodymyr Trofymenko**; simulation – **Maksym Peretiatko**; validation, formal analysis – **Volodymyr Trofymenko**, **Denys Kolesnikov**; writing – original draft preparation – **Volodymyr Pavlikov**; writing – review and editing – **Denys Kolesnikov**.

Conflict of interest

The authors declare that they have no conflict of interest in relation to this research, whether financial, personal, authorship or otherwise, that could affect the research and its results presented in this paper.

ISSN 1814-4225 (print)
ISSN 2663-2012 (online)

Financing

This study was conducted without financial support.

Data availability

The manuscript has no associated data.

Use of Artificial Intelligence

The authors confirm that they did not use artificial intelligence methods while creating the presented work.

All the authors have read and agreed to the published version of this manuscript.

References

1. Pavlikov, V., Zhyla, S., Pozdniakov, P., Kolesnikov, D., Cherepnin, H., Shmatko, O., Odokiienko, O., Malashta, P., & Tserne, E. Foundations of Radar Synthesis Theory of Phantom Objects Formation in SAR Images. *Radioelectronic and Computer Systems*, 2024, no. 3, pp. 123-140. DOI: 10.32620/reks.2024.4.11.

2. Pavlikov, V. V., Pozdniakov, P. V., Tserne, E. O., Kolesnikov, D. V., Peretiatko, M. S., & Malashta, P. P. Teoriya fantomizatsiyi radiozobrazhen' RSA: bazovi vidomosti ta obgruntuvannya rozmiriv dilyanky fantomizatsiyi [Theory of phantomization of SAR radio images: basic information and justification of phantomization area sizes]. *Aviatsiyno-kosmichna tekhnika i tekhnolohiya – Aerospace technic and technology*, 2024, no. 5, pp. 72-84. DOI: 10.32620/aktt.2024.5.08. (In Ukrainian).

3. Natale, A., Berardino, P., Esposito, C., & Pema, P. Airborne SAR for high resolution imaging. *Proceedings of the 2017 Joint Urban Remote Sensing Event (JURSE)*, Dubai, United Arab Emirates, IEEE, 2017, pp. 1-3. DOI: 10.1109/JURSE.2017.7924626.

4. Ferdowsi, B., Bhanu, M., Rao, C., Stieglitz, A., Loganathan, D., & Schubert, C. NASA-ISRO Synthetic Aperture Radar (NISAR): The Last Steps to Launch. *Proceedings of the 2024 IEEE Aerospace Conference*, Big Sky, MT, USA, IEEE, 2024, pp. 1-10. DOI: 10.1109/AERO58975.2024.10520949.

5. Chekka, A. B., & Aggala, N. J. High frequency Chirp signal generator using multi DDS approach on FPGA. *Proceedings of the 2021 5th International Conference on Trends in Electronics and Informatics (ICOEI)*, Tirunelveli, India, IEEE, 2021, pp. 137-142. DOI: 10.1109/ICOEI51242.2021.9453012.

6. *IEEE Std 1900.1-2019. IEEE Standard for Definitions and Concepts for Dynamic Spectrum Access: Terminology Relating to Emerging Wireless Networks, System Functionality, and Spectrum Management – Redline*. Piscataway, NJ, USA, IEEE, 2019, 144 p.

7. Souli, N., Stavrinides, S. G., Kardaras, P., Picos, R., Karatzia, M., & Kolios, P. Performance Evaluation of a Prototype UAV-Based Secure Communication System Employing ROS and Chaotic Communications. *Proceedings of the 2024 International Conference on Unmanned Aircraft Systems (ICUAS)*, Chania – Crete, Greece, IEEE, 2024, pp. 1034-1041. DOI: 10.1109/ICUAS60882.2024.10556964.

8. Šimon, O., Veselý, J., & Gabard, A. Single Channel Degarbling of SIF/IFF Pulses Using Spectral Inverse Filtering. *Proceedings of the 2023 24th International Radar Symposium (IRS)*, Berlin, Germany, IEEE, 2023, pp. 1-8. DOI: 10.23919/IRS57608.2023.10172453.

9. Kemp, D. A., King, S. C., Horne, N. C., Larsen, R. A., Garfield, I. R., & Santos. J. 300–900 MHz Midband Array Design for the Lunar Farside Technosignatures and Transients Telescope. *Proceedings of the 2025 United States National Committee of URSI National Radio Science Meeting (USNC-URSI NRSM)*, Boulder, CO, USA, IEEE, 2025, pp. 48-48. DOI: 10.23919/USNC-URSINRSM66067.2025.10906969.

10. Van Trees, H. L. *Detection, Estimation and Modulation Theory, Part I: Detection, Estimation, and Linear Modulation Theory*. John Wiley & Sons Inc, 2001. 697 p.

11. Cramér, H. *Mathematical Methods of Statistics*. Princeton University Press, 1946. pp. 367-369.

12. Skolnik, M. I. *Radar Handbook*. 3rd ed. McGraw-Hill, 2008. 1328 p.

13. Stoica, P., & Nehorai, A. On the concentrated stochastic likelihood function in array signal processing. *Circuits Systems and Signal Process*, 1995, no. 14, pp. 669-674. DOI: 10.1007/BF01213963.

14. Volosyuk, V. K., Zhyla, S. S., Antonov, M. O., & Khaleev, O. A. Optimal Acquisition Mode and Signal Processing Algorithm in Synthetic Aperture Radar. *Proceedings of the 2017 IEEE 37th International Conference on Electronics and Nanotechnology (ELNANO)*, Kyiv, Ukraine, IEEE, 2017, pp. 511–516. DOI: 10.1109/ELNANO.2017.7939804.

15. Xia, M., Gong, W., & Yang, L. A. Novel Waveform Optimization Method for Orthogonal-Frequency Multiple-Input Multiple-Output Radar Based on Dual-Channel Neural Networks. *Sensors*, 2024, vol. 24, no. 17, article no. 5471. DOI: 10.3390/s24175471.

16. Ahn, J., Lee, D.-H., Lee, S., & Kim, W. Frequency Shift Keying-Based Long-Range Underwater Communication for Consecutive Channel Estimation and Compensation Using Chirp Waveform Symbol Signals. *Journal of Marine Science and Engineering*, 2023, vol. 11, no. 9, article no. 1637. DOI: 10.3390/jmse11091637.

17. Serbes, A. On the Estimation of LFM Signal Parameters: Analytical Formulation. *IEEE Transactions on Aerospace and Electronic Systems*, 2018, vol. 54, no. 2, pp. 848-860. DOI: 10.1109/TAES.2017.2767978.

18. Aldimashki, O., & Serbes, A. LFM signal parameter estimation in the fractional Fourier domains: Analytical models and a high-performance algorithm. *Signal Processing*, 2024, vol. 214, article no. 109224. DOI: 10.1016/j.sigpro.2023.109224.

19. Zhai, G., Zhou, J., Yu, K., & Li, J. Chirp Rate Estimation of LFM Signals Based on Second-Order Synchrosqueezing Transform. *Electronics*, 2023, vol. 12, no. 24, article no. 4938. DOI: 10.3390/electronics12244938.

20. Wu, A. Y., Shi, X. Y., Sun, Y., Jiang, X., Qiang, S. Z., Han, P. Y., Chen, Y. J., & Zhang, Z. C. A Computationally Efficient Optimal Wigner Distribution in LCT Domains for Detecting Noisy LFM Signals. *Mathematical Problems in Engineering*, 2022, article no. 2036285. DOI: 10.1155/2022/2036285.

21. He, Y., & Zhang, Z. Symplectic Wigner Distribution in the Linear Canonical Transform Domain: Theory and Application. *IEEE Transactions on Signal Processing*, 2025, vol. 73, pp. 3688-3706. DOI: 10.1109/TSP.2025.3572739.

22. Shuo, M., Chen, M., Cheng, W., & Xiang, Y. A Method Based on Random Demodulator and Waveform Matching Dictionary to Estimate LFM Signal Parameter. *Journal of Sensors*, 2023, article no. 2499336. DOI: 10.1155/2023/2499336.

23. Meng, S., Meng, C., & Wang, C. Estimation of LFM signal parameters using RD compressed sampling and the DFRFT dictionary. *EURASIP Journal on Advances in Signal Processing*, 2023, article no. 93. DOI: 10.1186/s13634-023-01057-4.

24. Fei, S., Yan, M., Zhou, F., Wang, Y., Zhang, P., Wang, J., & Wang, W. A Parameter Estimation Method for Linear Frequency Modulation Signals Based on High-Resolution Spectral Line Representation. *Electronics*, 2025, vol. 14, no. 6, article no. 1121. DOI: 10.3390/electronics14061121.

25. Su, H., Bao, Q., & Chen, Z. Parameter Estimation Processor for Chirp Signals Based on a Complex-Valued Deep Neural Network. *IEEE Access*, 2019, vol. 7, pp. 176278-176290. DOI: 10.1109/ACCESS.2019.2957863.

Received 27.04.2025, Received in revised form 10.09.2025
Accepted date 17.11.2025, Published date 08.12.2025

ОЦІНЮВАННЯ ПАРАМЕТРІВ РАДІОІМПУЛЬСУ З ЛІНІЙНОЮ ЧАСТОТНОЮ МОДУЛЯЦІЄЮ

В. В. Павліков, М. С. Перетятько, В. М. Трофименко, Д. В. Колесніков

Предметом вивчення в статті є процес оцінювання параметрів імпульсного сигналу з лінійною частотною модуляцією (ЛЧМ), який використовується в бортових радіолокаційних системах, зокрема в радарах із синтезованою апертурою антени (РСА). **Метою** статті є синтез алгоритмів оптимального оцінювання основних параметрів ЛЧМ-сигналу (несучої частоти, швидкості зміни частоти модуляції, тривалості імпульсу та обвідної радіоімпульсу) і розроблення структурної схеми приймача радара, що реалізує такі алгоритми. **Завдання**, на вирішення яких спрямовано дослідження: побудувати математичну модель сигналу з лінійною частотною модуляцією, який випромінюється радаром, рівняння спостереження та функціонал правдоподібності; методом максимальної правдоподібності синтезувати алгоритми оцінювання параметрів ЛЧМ-сигналу; провести чисельне моделювання вихідних ефектів оцінювання відповідних параметрів ЛЧМ-сигналу; розробити структурну схему тракту приймача на основі синтезованих алгоритмів. Вирішення поставлених завдань ґрунтуються на **методах** статистичної теорії радіотехнічних систем та чисельного моделювання. Отримані наступні **результати**: 1) синтезовано алгоритми оцінювання несучої частоти, швидкості зміни частоти, тривалості імпульсу та обвідної радіоімпульсу; 2) проведене моделювання показало високу стійкість алгоритмів до шумів (до рівня сигнал/шум –30 dB); 3) побудовано структурну схему радара, що реалізує синтезовані алгоритми та забезпечує уточнення оцінюваних параметрів у зворотному зв’язку. **Висновки.** Наукова новизна отриманих результатів полягає в наступному: отримано алгоритми оцінювання параметрів як точкових (несуча частота, швидкість зміни частоти модуляції, тривалість імпульсу) так і часових характеристик (обвідна радіоімпульсу) імпульсних ЛЧМ-сигналів методом максимальної правдоподібності; вперше показано, що оцінювання ширини імпульсу вимагає розв’язання трансцендентного рівняння, а оцінювання обвідної – згладжування у ковзному вікні; отримані результати розширюють застосування методу максимальної правдоподібності в теорії оцінювання параметрів сигналів;

ISSN 1814-4225 (print)
ISSN 2663-2012 (online)

отримала подальший розвиток теорія фантомізації радіозображень у частині конструювання приймальних трактів радарів фантомізації.

Ключові слова: параметри імпульсу; лінійна частотна модуляція; метод максимальної правдоподібності; радар фантомізації; радар з синтезуванням апертури.

Павліков Володимир Володимирович – д-р техн. наук, проф., начальник, Державний Науково-Дослідний Інститут технологій кібербезпеки та захисту інформації, Київ, Україна.

Перетятько Максим Сергійович – технік, Державний Науково-Дослідний Інститут технологій кібербезпеки та захисту інформації, Київ, Україна.

Трофименко Володимир Михайлович – д-р юрид. наук, проф., заступник голови, Державна служба спеціального зв'язку та захисту інформації України, Київ, Україна.

Колесніков Денис Вікторович – д-р філософії, інженер, Державний Науково-Дослідний Інститут технологій кібербезпеки та захисту інформації.

Volodymyr Pavlikov – D.Sc., Professor, Chief of the State Scientific and Research Institute of Cybersecurity Technologies and Information Protection, Kyiv, Ukraine,
e-mail: v.pavlikov@khai.edu, ORCID: 0000-0002-6370-1758, Scopus Author ID: 23397933100.

Maksym Peretiatko – Technician at the State Scientific and Research Institute of Cybersecurity Technologies and Information Protection, Kyiv, Ukraine,
e-mail: peretiatko22@gmail.com, ORCID: 0000-0002-3536-5355, Scopus Author ID: 57981779800.

Volodymyr Trofymenko – D.Sc., Professor, Deputy Head of the State Service of Special Communications and Information Protection of Ukraine, Kyiv, Ukraine,
e-mail: tvm.stolica@gmail.com.

Denys Kolesnikov – PhD, Engineer at the State Scientific and Research Institute of Cybersecurity Technologies and Information Protection, Kyiv, Ukraine,
e-mail: d.kolesnikov@cip.gov.ua, ORCID: 0000-0002-0135-2695, Scopus Author ID: 57207915447.